Int. J. Electrochem. Sci., 8 **(2013)** 8774 - 8785

International Journal of
ELECTROCHEMICAL
SCIENCE
www.electrochemsci.org

Recognition and Electrochemical Determination of Environmental Contaminants Nitrophenol by Cyclodextrin Homologous Functionalized Graphene Modified Electrodes

Jianfei Xia[1], *Zonghua Wang*[1,*], *Xinmei Guo*[1], *Yanzhi Xia*[1,*], *Feifei Zhang*[1,2], *Jie Tang*[2], *Yanhui Li*[1], *Guangting Han*[1], *Linhua Xia*[1]

[1] Laboratory of Fiber Materials and Modern Textile, the Growing Base for State Key Laboratory, College of Chemical and Environment Engineering, Shandong Sino-Japanese Center for Collaborative Research of Carbon Nanomaterials, Qingdao University, Shandong, 266071, P. R. China.
[2] National Institute for Materials Science, Sengen 1-2-1, Tsukuba 305-0047, Japan
[*]E-mail: wangzonghua@qdu.edu.cn; qdxyzh@163.com

Received: 13 April 2013 / *Accepted:* 12 May 2013 / *Published:* 1 June 2013

The determination of Nitrophenol (NP) isomers, one type of serious environmental contaminants, is of great importance for environmental control. Herein, a novel electrochemically modified glassy carbon electrodes (CDs/CRG/GCE) is developed for determination of NP isomers using different cyclodextrins (α-, β- and γ-CD) in combination with chemically reduced graphene (CRG). The recognition mechanism of different cyclodextrins (CDs) for NP isomers is systematically studied. Interestingly enough, the cavity size of CDs plays an important role in the recognition of NP isomers. The α-CD/CRG/GCE and γ-CD/CRG/GCE display the best response to *p*-NP and *o*-NP, respectively. All three types of CDs modified electrodes show the similar effect on *m*-NP. Attributed to the synergistic effect of the specific recognition property of CDs and the excellent electronic property of CRG, the CDs/CRG/GCE exhibits outstanding supramolecular recognition and sensitive electrochemical response to NP isomers compared with that of CRG/GCE. The reductive peak current of *p*-NP at α-CD/CRG/GCE is linearly dependent on the concentration in the range from 1.0×10^{-7} to 1.5×10^{-4} mol/L with a low detection limit of 3.3×10^{-8} mol/L. The present work offers a new way to broaden the analytical applications of graphene-based materials for isomer analysis.

Keywords: Cyclodextrin; Graphene; Modified electrodes; Recognition; Determination; Isomer

1. INTRODUCTION

Nitrophenol (NP) isomers, including *o*-NP, *m*-NP and *p*-NP, are a type of serious environmental contaminants due to their toxicity and persistence. Among these isomers, *p*-NP is

considered as the most serious chemicals. These compounds exist not only in industrial wastewater, but also in freshwater and marine environments [1]. Therefore, the qualitative and quantitative detection of NP isomers, especially the selective detection of *p*-NP in the presence of *o*-NP and *m*-NP, become an important environmental analysis problem. Various methods such as spectrophotometry [2], chromatographic separation with spectrometry [3, 4], electrochemical methods [5, 6] have been used to the detection of *p*-NP. Among these methods, the electrochemical methods have been particularly advantageous owing to their unique properties of quick response, no need of expensive or large instrument, simple operation, and timesaving.

At present, graphene is one of the most widely used modifiers for electrochemical sensors owing to its unique nanostructure and unusual properties [7, 8]. Graphene, a single layer of carbon atoms in a closely packed honeycomb two-dimensional lattice, is a basic building block for graphitic materials of all other dimensionalities [9]. Because of those unusual characteristics including high surface area, excellent electrical, physical properties [10, 11] and potential low cost, graphene can be widely used in electronic devices [12, 13] such as lithium ion battery [14, 15], supercapacitor [16], and sensors [17, 18]. However, the poor dispersibility of graphene in solvents limits further applications. Graphene easily tends to agglomerate through Van der Waals interactions and strong π-π stacking [19]. For this reason, various reagents such as didodecyldimethylammonium bromide [20], poly-electrolytes [21, 22], chitosan [23], large aromatic molecules [24, 25], and cyclodextrins (CDs) [26] have been used to disperse or functionalize graphene. Among them, CDs are considered as a kind of desirable and excellent dispersive reagent due to their excellent film-forming ability and inclusion function.

With a lipophilic central cavity and a hydrophilic outer surface, CDs are cyclic oligosaccharides formed by joining α-D-glucopyranose units via α-1, 4-linkages. The unique properties can selectively allow the easy trapment of varieties of inorganic [27, 28], organic [29, 30] and biological guest molecules [31] into their hydrophilic cavities to form host-guest supramolecular complexes with molecular selectivity and enantioselectivity [32]. At the same time, since CDs are environmentally friendly and water-soluble, they have been widely used to improve the solubility and stability of functional materials and lipophilic compounds [33, 34]. Owing to the functionalization with CDs, the resulted graphene-nanohybrid is likely to possess both unique characteristics of high supramolecular recognition and enrichment capability toward target molecules [26, 35, 36]. Dong's group [37] prepared β-CD functionalized graphene nanosheets to develop a high-performance electrochemical sensor for ultrasensitive determination of carbendazim. Liu's group [36] fabricated an electrochemical sensor based on β-CD@chemically reduced graphene/Nafion composite film for rutin detection. As is previously demonstrated, graphene has the advantage as enhanced materials to fabricate the electrochemical sensing interface. In addition, the CDs/graphene nanohybrid modified electrode can not only enhance the electrochemical performance, but also selectively determine the similar active molecules like DA and AA which have near oxidation potential. However, to the best of our knowledge, the recognization and selectively determination of NP isomers using CDs/graphene-based modified electrodes is rarely reported.

Herein, to establish a new method to determine NP isomers, the novel electrochemically modified glassy carbon electrodes (CDs/CRG/GCE) were developed using different cyclodextrins (α-, β- and γ-CD) in combination with chemically reduced graphene (CRG). The analytical performance of

various modified electrodes (α-, β-, γ-CD/CRG/GCE) to NP isomers were investigated in detail. Furthermore, the recognition mechanisms of α-, β- and γ-CD to NP isomers were systematically studied. The selective determination of *p*-NP by α-CD/CRG/GCE in the presence of *o*-NP and *m*-NP was particularly demonstrated. The present work explored a new way to broaden the analytical applications of graphene-based materials for isomer analysis.

2. EXPERIMENTAL

2.1. Materials and reagents

α-, β-, γ- Cyclodextrin were obtained from Sigma-Aldrich (St. Louis, MO, USA). Nitrophenol isomers (*o*-, *m*-, *p*- nitrophenol) were obtained from Tianjin Reagent Factory (Tianjin, China). All reagents were of analytical-reagent grade. All solutions were prepared with doubly distilled water. Graphene (chemically reduced graphene, CRG) was prepared with graphite obtained from Qingdao Fujin Graphite Co., Ltd. (Qingdao, China).

2.2. Instruments

Cyclic voltammetry (CV) and differential pulse voltammetry (DPV) measurements were performed using a CHI 660C electrochemical workstation (Shanghai Chen Hua Instrument Co., Ltd., China) with a conventional three-electrode cell. A glassy carbon electrode (GCE) and the modified electrodes were used as the bare and working electrodes, respectively. A platinum wire was used as the auxiliary electrode. All the potentials quoted in this work were referred to a saturated calomel electrode (SCE) as the reference electrode. An S-4800 transmission electron microscopy (TEM, Hitachi, Japan) and JSM-6390LV scan electron microscopy (SEM, Japan) were used to observe the morphology of CRG and CDs/CRG, respectively.

2.3. Synthesis of CRG

CRG was prepared by reducing GO via the previously reported method [38]. Graphene oxide (GO) nanosheets were synthesized from natural graphite by a modified Hummers' method [39]. The as-prepared GO was then dispersed in water (0.5 mg/mL) and centrifuged to obtain a brown homogeneous GO dispersion. Then, 3.5 mL of hydrazine solution and 40.0 mL of ammonia solution were added into the dispersion. After being vigorously shaken or stirred for a few minutes, the vial was incubated at 95 °C for 1 h. The black CRG precipitation was then obtained by filtration and successively washing with doubly distilled water and methyl alcohol. Finally, the prepared CRG was dried in vacuum at 60 °C overnight.

2.4. Preparation of modified electrodes

Prior to use, the bare glassy carbon electrode (GCE) was polished to a mirror-like surface with 0.3 and 0.05 μm Al_2O_3 slurry on emery paper, followed by rinsing with doubly distilled water and sonication in 1:1 nitric acid, acetone and doubly distilled water for 10 min, respectively.

As-synthesized CRG was dispersed in CDs aqueous solution (2 wt. %) to form a 0.1 mg/mL homogeneous suspension (CDs/CRG) by sonication. The CDs/CRG/GCE were prepared by dropping 6.0 μL of the CDs/CRG suspension on the GCE surface and evaporating the remaining water using an infrared lamp. In comparison with the CDs/CRG/GCE, the CRG/GCE was prepared by coating CRG water suspension on GCE.

3. RESULTS AND DISCUSSION

3.1. Morphological Characterization

Fig. 1 A shows the TEM image of the CRG. As was can be seen, the as-prepared CRG showed a typical flake-like shape of graphene. The thickness was about 2~3 nm with few-layer graphene as reported in our previous work [40]. The morphology of the α-CD/CRG was characterized by SEM shown in Fig. 1 B. The surface of the α-CD/CRG was rough and nonuniform. The graphene prepared through chemically reduced method have some -OH groups, which can form strong hydrogen bonding with the CDs. Hence, the CD molecules were covered on the surface of CRG, which could prevent the coalescence and aggregation of graphene. Moreover, it can be demonstrated that the CD/CRG nanohybrid dispersed well in water.

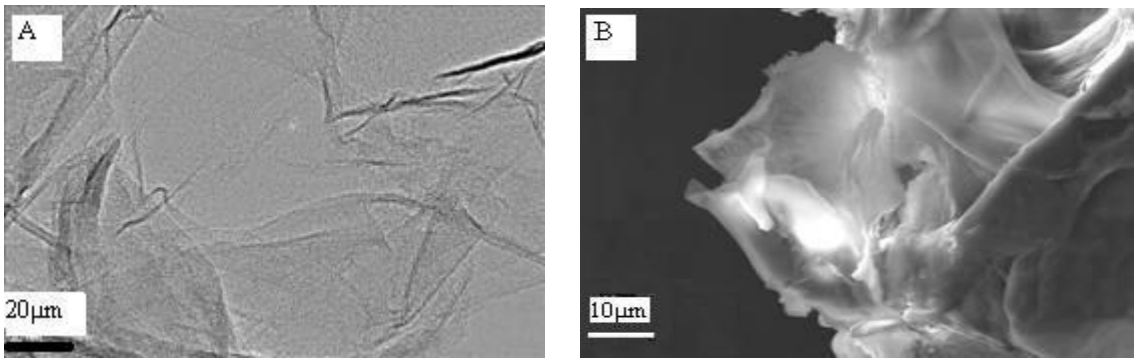

Figure 1. TEM of CRG (A); SEM of α-CD/CRG (B).

3.2. Electrochemical Behavior of p-NP at α-CD/CRG/GCE

The electrochemical behavior and reaction mechanism of *p*-NP at the α-CD/CRG/GCE were demonstrated. Fig. 2A shows the continuous CVs of 1.0×10^{-4} mol/L *p*-NP at α-CD/CRG/GCE in PBS buffer (pH 6.5). As a comparison, curve c is the CV of α-CD/CRG/GCE in the PBS buffer, we can see there was no redox peaks in the blank solution. Curve a and curve b are the successive CV scan curves

in the presence of 1.0×10^{-4} mol/L *p*-NP. In the first cycle (curve a), a reductive peak (A_1) appeared at -0.717 V in the cathodic sweep corresponding to the reduction of *p*-NP. Meanwhile, another peak appeared at +0.156 V (B) in the anodic sweep.

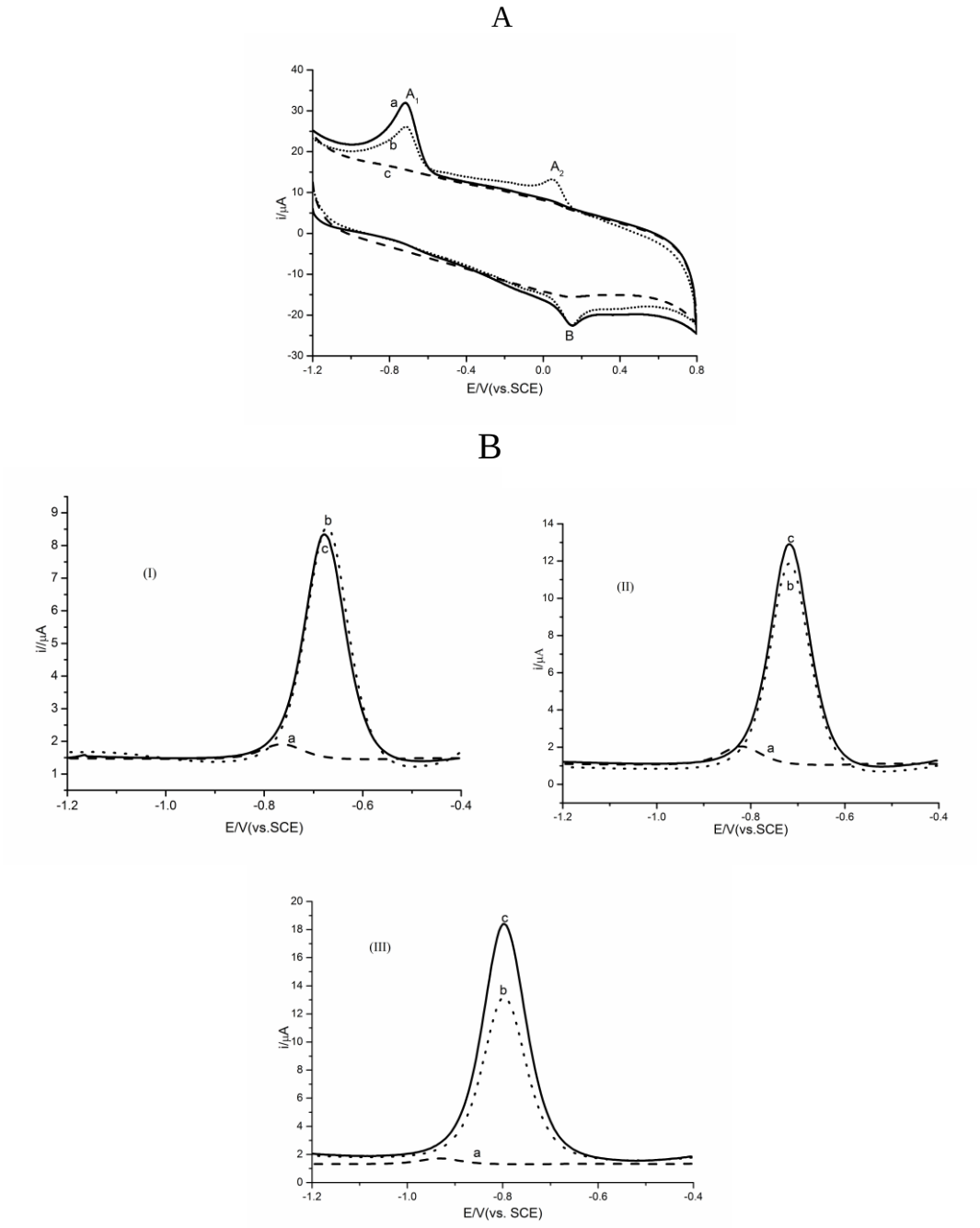

Figure 2. The behavior of *o*-NP, *m*-NP and *p*-NP at modified electrodes. (A) CVs of *p*-NP at α-CD/CRG/GCE. The first scan (a, solid line), the second scan (b, dot line) and without *p*-NP (c, dash line) in pH 6.5 PBS at 100 mV/s; (B) DPVs of *o*-NP (I), *m*-NP (II) and *p*-NP (III) at bare GCE (a, dash line), CRG/GCE (b, dot line) and α-CD/CRG/GCE (c, solid line). PBS pH 6.5, $C_{NP}=1.0\times10^{-4}$ mol/L.

In the following cycle (curve b), in addition to the A_1 peak, a new reductive peak (A_2) was observed at +0.044 V. It was interesting that the peak current of reversible couple (A_2/B) increased while the irreversible peak current (A_1) decreased. It was evident that the products of *p*-NP by irreversible reduction remained on or near to the modified electrode surface, which was oxidized on the anodic sweep. When the scan potential changed in the range of 0.8 to -0.4 V, the redox couple peaks disappeared gradually. These interesting phenomena demonstrate that the development of A_1 peak is responsible for the formation of A_2 and B peaks.According to the literature [41], a similar reaction mechanism of *p*-NP at α-CD/CRG/GCE in aqueous media is given in the following:

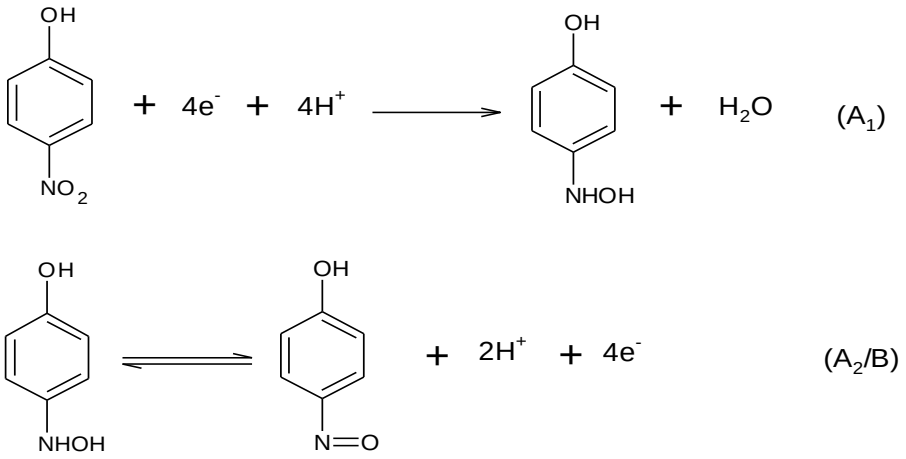

3.3. The Recognition Ability of Various CDs/CRG/GCE for NP Isomers

To investigate the analytical performance of the obtained CDs/CRG/GCE, DPV was used to study the amperometric response to NP isomers using their irreversible reduction peak of A_1. Fig. 2B shows the typical DPVs of *o*-NP, *m*-NP, and *p*-NP at bare GCE, CRG/GCE and α-CDs/CRG/GCE, respectively. NP isomers demonstrated broad and small reductive peaks at bare GCE (curve a), while lead to good and spiky reductive peaks at less negative potential at the CRG/GCE and α-CD/CRG/GCE. The reductive peak potential, *E*p, shifted about 90~140 mV positively compared with that of bare GCE. In addition, the peak current increased 5~10 times than that on bare GCE. The similar phenomena were also found at β-CD/CRG/GCE and γ-CD/CRG/GCE as shown in Table 1.

Table 1. The recognition ability of various CDs/CRG/GCE for NP isomers

Electrodes	*i*(μA)			E_p(V)		
	o-NP	*m*-NP	*p*-NP	*o*-NP	*m*-NP	*p*-NP
Bare GCE	1.91	2.03	1.72	-0.764	-0.824	-0.932
CRG/GCE	8.56	11.86	13.19	-0.676	-0.716	-0.796
α-CD/CRG/GCE	8.33	12.90	18.40	-0.676	-0.716	-0.796
β-CD/CRG/GCE	11.10	12.12	15.65	-0.648	-0.732	-0.800
γ-CD/CRG/GCE	15.89	12.83	14.27	-0.572	-0.732	-0.804

In comparison with the current signal of three NP isomers at the bare GCE, it can be found the current values ($\triangle i$) of all were increased but the degree is different at the CRG/GCE, $\triangle i_p \approx \triangle i_m > \triangle i_o$, suggesting that CRG/GCE has similar strong catalysis to *m*-, *p*-NP, but mild action to *o*-NP. These can be explained as follows. CRG as a support can enhance the electron transfer from target molecules to electrode due to its subtle electronic property. In addition, due to its huge surface area, NP isomers could be accumulated on the surface of CRG through π-π conjugate and hydrogen-bonding interactions. Thus, dramatical improvement in its sensitivity for NP isomers at the CRG/GCE is obtained as expected. However, *o*-NP has the similar spatial structure as naphthaline resulting in intramolecular hydrogen-bonding interaction while reducing intermolecular hydrogen-bonding interaction between *o*-NP and CRG. Such a structure of *o*-NP makes it no easy to be close the active surface of the CRG/GCE. Consequently, the current of *o*-NP at CRG/GCE increased more slightly than the case of *m*-NP and *p*-NP. On the other hand, the shift of peak potential ($\triangle E_p$) of NP isomers was difference at CRG/GCE compared with the bare GCE, $\triangle E_{pp} > \triangle E_{pm} > \triangle E_{po}$, which indicated that the spatial structure effect lead to the different orientation manner of NP isomers towards the surface of modified electrode.

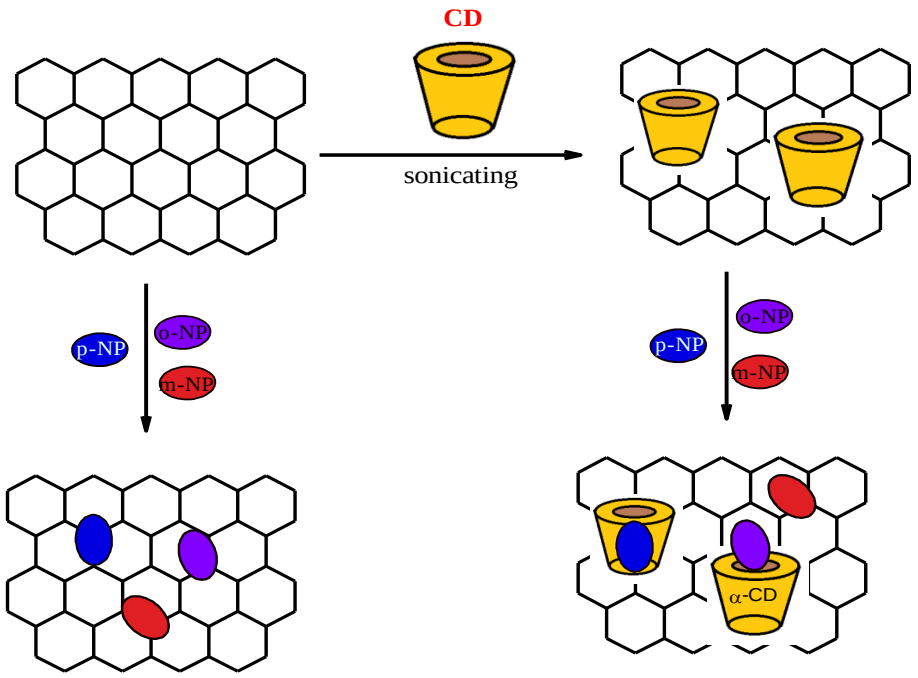

Figure 3. Illustration of the procedure for α-CD/CRG/GCE and CRG/GCE sensing the guest molecules by an electrochemical strategy.

Figure 3 shows the illustration of the procedure for CRG/GCE and α-CD/CRG/GCE sensing the guest molecules (*o*-, *m*- and *p*-NP) by an electrochemical strategy. CD molecules are able to accommodate guest molecules (NP isomers) fitting their spatially to form host-gust complex with high supramolecular recognition capability. The CD existence on the CRG/GCE play a important role for the recognition of NP isomers. Table 1 shows that the peak currents of NP isomers increase at CDs/CRG/GCE compared to CRG/GCE and bare GCE, indicating a favorable catalytic activity of nanohybrid CDs/CRG toward NP isomers. The CDs functionalized CRG possessed high

supramolecular recognition capability and show the selectivity towards NP isomers. The ability of forming inclusion complexes between NP isomers and CDs is depending on the molecular structure, size, and hydrophobility.

In the case of α-CD/CRG/GCE, the peak current of *p*-NP increased significantly owning to its linear symmetry, which could be easily trapped into CD's inner cavity to form inclusion complexes. However, *o*- and *m*-NP were not very easy to be encapsulated into CD's inner cavity owing to their steric effect. These results suggested that the CDs/CRG nanohybrid not only showed excellent properties of CRG but also exhibited supramolecular recognition capability of CDs. Moreover, CDs were modified on the surface of the GCE resulting a homogeneous film of CDs/CRG, which facilitated the construction of reproducible electrodes with high sensitivity.

3.4. The Effect of Cavity Size of CDs on Recognition

It is well known that the cavity diameter of α-, β- and γ-CD increases gradually (0.57, 0.78, 0.95 nm, respectively). Based on the results in Table 1, it was clearly presented that the three kinds of electrodes (α-, β- and γ-CD/CRG/GCE) have different response to NP isomers. Taking *o*-NP as an example, the response peak current at α-, β- and γ-CD/CRG/GCE (i*o*α, i*o*β and i*o*γ, respectively) was different, i*o*γ (15.89 μA)>i*o*β (11.10 μA)>i*o*α (8.33 μA), which suggested that the cavity size of γ-CD was more perfectly fit to the special size of *o*-NP. Based on the steric size of *p*-NP, m-NP and o-NP increases gradually, γ-CD/CRG/GCE owing the biggest cavity size presented the best catalysis for *o*-NP, α-CD/CRG/GCE owing the smallest cavity size showed the best catalysis for *p*-NP, while three types of CDs/CRG/GCE had the similar effect on *m*-NP. On the other hand, compared with CRG/GCE, the shift of peak potential of NP isomers at CDs/CRG/GCE were also different. In the case of *o*-NP, it is found that the peak potential shift was negligible at α-CD/CRG/GCE, while shifted to a positive value gradually at β- and γ-CD/CRG/GCE compared with that at CRG/GCE. For the case of *m*-NP, the peak potential at α-CD/CRG/GCE presented no shift, while its shifted a same value at β- and γ-CD/CRG/GCE. However, the peak potential of *p*-NP showed a negligible change at three types of CDs/CRG/GCE. It was noteworthy that the results basically illuminated the size fit rule for the CD inclusion complex.

3.5. Determination of p-Np at the α-CD/CRG/GCE

In order to demonstrate the sensing performance of the α-CDs/CRG/GCE toward NP isomers, DPVs of *o*-NP, *m*-NP, *p*-NP and their mixed solution at the α-CD/CRG/GCE are shown in Fig. 4A. From the complete coincidence of *p*-NP DPVs in single and mixed solution, it can be illustrated that the presence of *o*-NP and *m*-NP had no interference to the selective determination of *p*-NP. The results fully demonstrated that the α-CD/CRG/GCE had favorable recognition towards *p*-NP and can lead to its highly sensitive and selective determination.

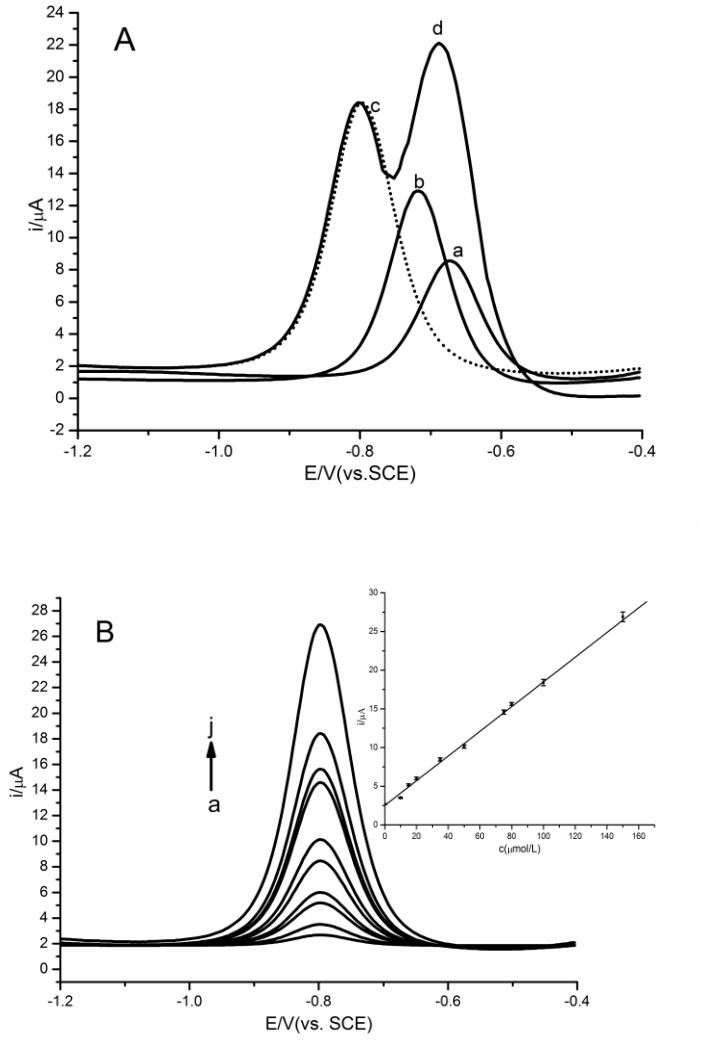

Figure 4. Determination of *p*-NP. (A) DPVs of a) *o*-NP, b) *m*-NP, c) *p*-NP, d) mixed NP isomers at α-CD/CRG/GCE (C_{NP}=1.0×10^{-4} mol/L); (B) DPVs of different concentrations of *p*-NP at α-CD/CRG/GCE. $C_{p\text{-NP}}$ (a~j): 0.1, 10, 15, 20, 35, 50, 75, 80, 100 and 150 (μmol/L), Inset: concentration calibration curve of the DPV current response for *p*-NP. PBS 6.5, accumulation time 60s.

The determination of *p*-NP was carried out at α-CD/CRG/GCE. Fig. 4B shows the typical DPVs obtained from different concentrations of *p*-NP. Under the optimal conditions, the peak currents had a good linear relationship with the *p*-NP concentration in the range of 1.0 × 10^{-7} to 1.5 × 10^{-4} mol/L. The linear regression equation was *i* (μA)=0.162 C (μmol/L) + 2.191, with a correlation coefficient (R) of 0.999. The detection limit (S/N = 3) was estimated to be about 3.3 × 10^{-8} mol/L, which was lower than that obtained on a carbon nanotube electrode (4.0 × 10^{-7} mol/L) [41] and a hydroxyapatite nanopowder modified electrode (6.0 × 10^{-7} mol/L) [42]. The lower detection limit could be attributed to the combination of α-CD and CRG, in which the α-CD can selectively hold the *p*-NP and the CRG provided a large specific surface area to increase the loading of *p*-NP and α-CD. In

addition, the CRG could accelerate the electron transfer on the electrode surface to amplify the electrochemical signal due to the outstanding electronic conductivity of CRG.

The α-CD/CRG/GCE was applied to the detection of *p*-NP in lake water (collected from Qingdao, China) using the above method. No signal for *p*-NP was observed in the water samples. Thus, the determination of *p*-NP concentration was performed by the standard addition method and the results are listed in Table 2. The recoveries of this method are in the range from 96.7% to 102.4%, which indicated that this method was reliable, effective and sufficient for the *p*-NP determination. Additionally, the interferences from other NP isomers in water samples can be almost neglected.

Table 2. Determination of *p*-NP in lake water sample

	Added ($\times10^{-5}$ mol/L)	Found ($\times10^{-5}$ mol/L)	RSD (%)	Recovery (%)
Lake Water	0.00	0.00	0	0
	5.00	5.12	3.45	102.4
	10.00	9.67	2.32	96.7
	15.00	14.78	2.01	98.5

4. CONCLUSIONS

To establish a reliable method for determination of NP isomers, novel electrochemically modified glassy carbon electrodes CDs/CRG/GCE were developed using cyclodextrins in combination with chemically reduced graphene. The cavity size of CDs played an important role in the recognition of NP isomers. Attributed to the synergistic effect of the specific recognition property of CDs and the excellent electronic property of CRG, CDs/CRG/GCE exhibited outstanding supramolecular recognition and sensitive electrochemical response to NP isomers. Selective determination of *p*-NP in the presence of *o*-NP and *m*-NP could be realized with low detection limit and good anti-interference ability using the modified electrode. The present work offered a new way to broaden the analytical applications of graphene-based materials in isomer analysis.

ACKNOWLEDGEMENTS

This work was financially supported by National Natural Science Foundation of China (authorized number: 20975056, 21275082 and 81102411), the Natural Science Foundation of Shandong (ZR2011BZ004, ZR2011BQ005), JSPS and NSFC under the Japan-China Scientific Cooperation Program (21111140014), the State Key Laboratory of Analytical Chemistry for Life Science (SKLACLS1110) and the National Key Basic Research Development Program of China (973 special preliminary study plan, Grant no.: 2012CB722705).

References

1. X. M. Lü, Z. W. Wu, J. Y. Shen, J. Feng, Y. T Wang, Y. Z. Song, *Int. J. Electrochem. Sci.*, 8 (2013) 2229.
2. A. Niazi, A. Yazdanipour, *J. Hazard Mater.*, 146(2007) 421.
3. M. J. Thompson, S. E. Cross, M. S Roberts, L. N. Ballinger, *J. Chromatogr*. B, 677(1996) 117.
4. M. Salman, M. S. Refat, I. Grabchev and A. M. A. Adam, *Int. J. Electrochem. Sci.*, 8 (2013) 2863.
5. Y. L. Yang, B. Unnikrishnan, S. M. Chen, *Int. J. Electrochem. Sci.*, 6**(2011)** 3902.
6. T. Ndlovu, O. A. Arotiba, R. W. Krause, B. B. Mamba, *Int. J. Electrochem. Sci.*, 5**(2010)** 1179.
7. V. Singh, D. H. Joung, L. Zhai, S. Das, S. I. Khondaker, S. Seal, *Prog. Mater. Sci*., 56(2011) 1178.
8. D.Chen, L. H.Tang, J. H Li, *Chem. Soc. Rev*., 39(2010) 3157.
9. A. K.Geim, K. S.Novoselov, *Nat. Mater*., 6(2007) 183.
10. C. N. R. Rao, A. K. Sood, *Angew. Chem. Int. Ed.*, 48(2009) 7752.
11. S. Cheemalapati, S. Palanisamy, S. M. Chen, *Int. J. Electrochem. Sci*., 8 (2013) 3953.
12. B. Ntsendwana, B.B. Mamba, S. Sampath, O.A. Arotiba, *Int. J. Electrochem. Sci.*, 7**(2012)** 3501.
13. F. Chen, Q. Qing, J. L. Xia, J. H. Li, N. J. Tao, *J. Am. Chem. Soc*., 131(2009) 9908.
14. S.Y. Liu, J. Xie, Q. Pan, C. Y. Wu, G. S. Cao, T. J. Zhu, X. B. Zhao, *Int. J. Electrochem. Sci*., 7 (2012) 354.
15. B. Feng, J. Xie, G. S. Cao, T. J. Zhu, X. B. Zhao, *Int. J. Electrochem. Sci*., 7(2012) 5195.
16. X. L. Li, H. F. Song, Y. L. Zhang, H. Wang, K. Du, H. Y, Li, Y. Yuan, J. M. Huang, *Int. J. Electrochem. Sci.*, 7(2012) 5163.
17. Z. J. Zhuang1, J. Y. Li, R. Xu, D. Xiao, *Int. J. Electrochem. Sci.*, 6(2011) 2149.
18. D. Chen, J. H. Li, *Chem. Rev.*, 112(2012) 6027.
19. H. Rashedi, P. Norouzi, M. R. Ganjali, *Int. J. Electrochem. Sci.*, 8 (2013) 2479.
20. Y. Y. Liang, D. Q. Wu, X. L. Feng, K. Müllen, *Adv. Mater*., 21(2009) 1679.
21. Q. Zhang, S.Y. Wu, L. Zhang, J. Lu, V. Francis, Y. Liu, Z. Q. Xing, J. H. Li, X. M. Song, *Biosens. Bioelectron*., 26(2011) 2632.
22. H. Liu, J. Gao, M. Q. Xue, N. Zhu, M. N. Zhang, T. B. Cao, *Langmuir*, 25(2009) 1206.
23. Y. Wang, Y. M. Li, L. H. Tang, J. Lu, J. H. Li, *Electrochem. Commun*., 11(2009) 889.
24. Q. Zhang, Y. Qiao, F. Hao, L. Zhang, S. Y. Wu, Y. Li, J. H. Li, X. M. Song, *Chem. Eur. J.*, 16(2010) 8133.
25. Q.Su, S. P. Pang, V. Alijani, C. Li, X. L. Feng, K. Müllen, *Adv. Mater*., 21(2009) 3091.
26. Y. J. Guo, S. J. Guo, J. T. Ren, Y. M. Zhai, S. J. Dong, E. K. Wang, *ACS NANO*, 4(2010) 4001.
27. M. L. Brusseau, X. J. Wang, W. Z. Wang, *Environ. Sci. Technol*., 31 (1997) 1087.
28. M. E. Skold, G. D. Thyne, J. W. Drexler, D, L. Macalady, J. E. McCray, *Environ. Sci. Technol*., 42(2008) 8930.
29. B. Pekec, A. Oberreiter, S. Hauser, K. Kalcher, A. Ortner, *Int. J. Electrochem. Sci.*, 7 (2012) 4089.
30. Y. Liu, S. Z. Kang, H. Y. Zhang, *Microchem. J.*, 70(2001) 115.
31. F. Wang, G. K. Morteza, *Anal. Chem*., 68(1996) 3460.
32. S. N. Kikandi, V. A. Okello, Q. Wang, *Environ. Sci. Technol*., 45(2011) 5294.
33. R. Sawicki, L. Mercier, *Environ. Sci. Technol.*, 40(2006) 1978.
34. D. Y. Wang, L. L. Sun, W. Liu, W. W. Chang, X. Gao, Z. X. Wang, *Environ. Sci. Technol*., 43 (2009) 5825.
35. L. Tan, K. G. Zhou, Y. H. Zhang, H. X. Wang, X. D. Wang, Y. F. Guo, H. L. Zhang, *Electrochem. Commun*., 12(2010) 557.
36. K. P. Liu, J. P. Wei, C. M. Wang, *Electrochim. Acta*, 56(2011**)** 5189.
37. Y. J. Guo, S. J. Guo, J. Li, E. K. Wang, S. J. Dong, *Talanta*, 84(2011) 60.
38. Z. H. Wang, J. F. Xia, L. Y. Zhu, X. Y. Chen, F. F. Zhang, S. Y. Yao, Y. H. Li, Y. Z. Xia, *Electroanal.*, 23(2011) 2463.

39. N. I. Kovtyukhova, P. J. Ollivier, B. R. Martin, T. E. Mallouk, S. A. Chizhik, E. V. Buzaneva, A. D. Gorchinskiy, *Chem. Mater*., 11(1999) 771.
40. Z. H. Wang, J. F. Xia, L. Y. Zhu, F. F. Zhang, X. M. Guo, Y. H. Li, Y. Z. Xia, *Sensor. Actuat B: Chem*., 161(2012) 131.
41. L. Q. Luo, X. L. Zou, Y. P. Ding, Q. S. Wu, *Sensor. Actuat B: Chem*., 135(2008) 61.
42. H. S. Yin, Y. L. Zhou, S. Y. Ai, X. G. Liu, L. S. Zhu, L. N. Lu, *Microchim. Acta*, 169(2010) 87.